

Energy Cooperation Optimization in Microgrids with Renewable Energy Integration

Katayoun Rahbar, *Member, IEEE*, Chin Choy Chai, *Member, IEEE*, and Rui Zhang, *Senior Member, IEEE*

Abstract—Microgrids are key components of future smart grids, which integrate distributed renewable energy generators to efficiently serve the load locally. However, the intermittent nature of renewable energy generations hinders the reliable operation of microgrids. Besides the commonly adopted methods such as deploying energy storage system (ESS) and supplementary fuel generator to address the intermittency issue, *energy cooperation* among microgrids by enabling their energy exchange for sharing is an appealing new solution. In this paper, we consider the energy management problem for two cooperative microgrids each with individual renewable energy generator and ESS. First, by assuming that the microgrids' renewable energy generation/load amounts are perfectly known ahead of time, we solve the *off-line* energy management problem optimally. Based on the obtained solution, we study the impacts of microgrids' energy cooperation and their ESSs on the total energy cost. Next, inspired by the off-line optimization solution, we propose *online* algorithms for the real-time energy management of the two cooperative microgrids. It is shown via simulations that the proposed online algorithms perform well in practice, have low complexity, and are also valid under arbitrary realizations of renewable energy generations/loads. Finally, we present one method to extend our proposed online algorithms to the general case of more than two microgrids based on a clustering approach.

Index Terms—Microgrid, energy cooperation, renewable energy, distributed storage, smart grid, optimization.

I. INTRODUCTION

The increasing electric energy consumption in recent decades has become a serious concern for the existing power grids. To reduce both the operational and environmental costs of conventional fossil fuel based energy generations, microgrid that consists of networked groups of renewable energy generators and distributed loads has emerged as an appealing solution [1]. However, unlike the conventional energy generations, renewable energy is intermittent in nature; hence, it does not ensure the reliable operation of microgrids at all time.

To overcome the aforementioned issue, various approaches have been proposed in the literature. For instance, microgrids can be always connected to the main grid to meet their energy deficit. This approach is not environmentally friendly and may also lead to high energy cost for microgrids, since any energy deficit needs to be mitigated through drawing conventional energy from the main grid even when electricity prices offered by the main grid are high. On the other

hand, energy storage systems (ESSs) can be deployed in conjunction with renewable energy generators to store the energy surplus and be discharged upon energy deficit or when electricity prices offered by the main grid are high [2]. However, relying solely on ESSs is not a viable solution due to their limited capacities, high maintenance costs, and losses during charging/discharging [3]. With the advances in smart grid technologies, *energy cooperation* among microgrids has been proposed as a promising new solution to achieve the reliable and cost-effective operation of microgrids [4]. Energy cooperation enables microgrids with energy surplus to share energy to those with energy deficit. In addition, it reduces the overall transmission losses, since the distance among microgrids in the distribution network is practically smaller than that among microgrids and distributors in the main grid. Last but not least, it can reduce the need for large-size ESSs. However, it is important to optimize the amount of energy exchanged among microgrids, that drawn from the main grid by each microgrid, and that charged/discharged to/from the ESS of each microgrid. This optimization requires joint *energy management* of the microgrids.

It is worth nothing that there have been a handful of prior studies on the energy management problem for microgrids [5]–[21]. For instance, [5]–[7] studied the system with only a single microgrid or multiple microgrids operating independently without energy cooperation. The general case of joint energy management for multiple microgrids was considered in [8]–[21]. Specifically, [8]–[11] studied the off-line energy management problem by assuming that renewable energy generation/load amounts are either deterministic or known ahead of time. On the other hand, [12]–[21] solved the online energy management problem under the assumption of stochastic renewable energy generation/load models. However, the minimum and maximum constraints for the state of ESS were not considered in [12], [13]; therefore, their obtained results may not be practically implementable. In [14], ESS was not modeled in the system for simplicity. Furthermore, the renewable energy generation/load were assumed to either follow stationary processes [15] or their exact distributions were known [12], [16]–[18], which may not be practically valid for highly intermittent renewable energy sources such as solar. Besides, the online energy management problem was studied in [19] under the simplified model of no energy exchange between microgrids, and in [13], [20] under the assumption of ideal transmission lines without energy transmission losses. It is also noted that energy cooperation between the base stations with individual renewable energy generation in wireless communication systems was studied in [22].

K. Rahbar is currently with Solar Energy Research Institute of Singapore (SERIS), National University of Singapore (e-mail: k.rahbar@u.nus.edu).

C. C. Chai is with the the Institute for Infocomm Research, A*STAR, Singapore (e-mail: chaicc@i2r.a-star.edu.sg).

R. Zhang is with the Department of Electrical and Computer Engineering, National University of Singapore (e-mail: elezhang@nus.edu.sg). He is also with the Institute for Infocomm Research, A*STAR, Singapore.

In this paper, we investigate the real-time energy management problem for a system with two cooperative microgrids that belong to the same entity or different entities with common interests. We assume that the microgrids can exchange energy via the transmission line connecting them, and each comprises renewable energy generators, ESS, and an aggregate load. The main results of this paper are summarized as follows:

- We first formulate the *off-line* energy management problem by assuming that the microgrids' net energy profiles, i.e., the renewable energy generation offset by the aggregate load of individual microgrids, are perfectly known ahead of time. We then study the impacts of microgrids' energy cooperation and their ESSs on the total energy cost saving via simulations based on the real wind generation data of Tuscon power system [23]. The results show that although both energy cooperation and ESSs can be used to save the energy cost, one can be more effective than the other depending on the system setup. For instance, energy cooperation reduces the total energy cost more considerably when the microgrids' net energy profiles are highly uncorrelated. However, ESSs reduce the total energy cost more effectively when the net energy profiles are correlated and/or the energy loss in the transmission line is high.
- Next, we consider the practical setup of stochastic net energy profiles. Based on the results obtained from the off-line optimization, we propose two *online* algorithms of low complexity for the real-time cooperative energy management of microgrids, namely *store-then-cooperate* and *cooperate-then-store*. The proposed algorithms can be applied under arbitrary realizations of microgrids' net energy profiles. Simulation results reveal that our online algorithms perform very close to the optimal solution derived from the off-line optimization.
- Finally, we extend our proposed online algorithms to the general case of more than two microgrids based on a clustering approach. We show that the proposed clustering based approach performs fairly close to the optimal off-line solution, with performance losses of only 4.78% and 6.14% in the noisy environment with 15% and 30% renewable energy prediction errors, respectively.

In contrast to the prior works [5]–[21], in this paper we consider a more practical setup of cooperative microgrids with both renewable energy integration and deployment of ESSs, while adopting a practical model for energy sharing losses. In particular, we devise new online algorithms for the real-time energy management of cooperative microgrids, which i) achieve close-to-optimal performance in practice, ii) have low complexity as compared to stochastic gradient based methods in e.g., [15], and iii) are valid under arbitrary realizations of net energy profiles, unlike those in e.g., [16]–[18] assuming their known stochastic distributions. Compared to our previous work [5] that studied the energy management problem for a single microgrid, this paper studies microgrids' energy cooperation and its impact on the energy cost saving as well as reducing the need for bulk ESSs. A preliminary conference version of this work is presented in [24].

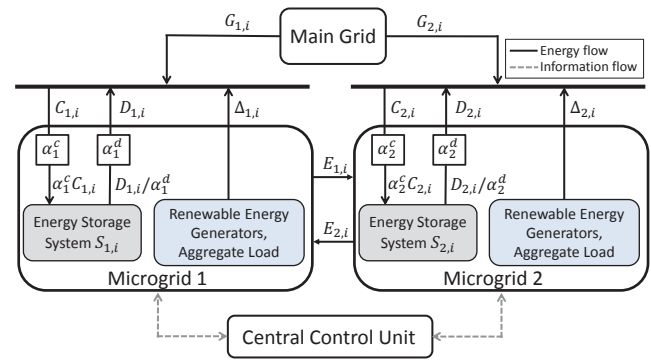


Fig. 1. System model.

The rest of this paper is organized as follows. Section II presents the system model. Section III presents the optimal solution to the off-line energy management problem and investigates the impacts of microgrids' energy cooperation and use of ESSs on the total energy cost. Section IV presents online algorithms for the real-time cooperative energy management of two microgrids. Section V presents one method to extend the proposed online algorithms to the general case of more than two microgrids. Last, we conclude the paper in Section VI.

II. SYSTEM MODEL AND PROBLEM FORMULATION

We consider a power system consisting of two microgrids that are connected to each other and also to the main grid, as shown in Fig. 1. Particularly, each microgrid, denoted by index j , $j \in \mathcal{J} = \{1, 2\}$, comprises renewable energy generators, an ESS, and an aggregate load. The two microgrids exchange energy via the transmission line connecting them, where the energy cooperation is coordinated by a central control unit that gathers the required information from both microgrids. We assume that the microgrids belong to the same entity or different entities with common interests. Hence, the central control unit jointly optimizes the energy exchanged between microgrids, that drawn from the main grid by each microgrid, and that charged/discharged to/from ESS of each microgrid to minimize their total energy cost over time. Note that the two microgrids cannot be treated as a single microgrid with simply aggregated energy generation and consumption, since the distance between microgrids is practically large and the transmission loss between them is considerable. However, the transmission losses within each microgrid are neglected due to their relatively smaller distance; hence, the renewable energy generation and load of each microgrid are aggregated, as shown in Fig. 1.

We assume a time-slotted system with slot index i , $i \in \mathcal{N} = \{1, \dots, N\}$, where $N \geq 1$ denotes the total number of time slots for energy management. For the convenience of analysis, we assume a quasi-static time-varying energy model, in which the rates of the renewable energy generation and load are constant within each time slot, but may change from one slot to another. We also assume that the duration of each slot is normalized to a unit time; hence, we can use power and energy interchangeably throughout this paper.

In the following, we define our system model in more detail.

1) *Energy Storage System (ESS)*: We denote the energy charged (discharged) to (from) the ESS of microgrid j at time slot i as $C_{j,i} \geq 0$ ($D_{j,i} \geq 0$). The energy losses during the charging and discharging processes are specified by the charging and discharging efficiency parameters, denoted by $0 < \alpha_j^c < 1$ and $0 < \alpha_j^d < 1$, respectively. Denote the state (stored energy) of the ESS of microgrid j at the beginning of time slot i as $S_{j,i} \geq 0$. The storage over time for microgrid j is then obtained as $S_{j,i+1} = S_{j,i} + \alpha_j^c C_{j,i} - D_{j,i}/\alpha_j^d$, $\forall i \in \mathcal{N}$. Moreover, we denote $S_j^{\max} \geq 0$ and $S_j^{\min} \geq 0$ as the storage capacity and the minimum energy allowed in the ESS of microgrid j , respectively. We thus have the following constraints for the states of the ESS in microgrid j :

$$S_j^{\min} \leq S_{j,1} + \alpha_j^c \sum_{k=1}^i C_{j,k} - 1/\alpha_j^d \sum_{k=1}^i D_{j,k} \leq S_j^{\max}, \forall i \in \mathcal{N} \quad (1)$$

where $S_j^{\min} \leq S_{j,1} \leq S_j^{\max}$, $\forall j \in \mathcal{J}$.¹

2) *Energy Cost of Microgrids*: We consider a linear time-varying energy cost model for the conventional energy drawn from the main grid [25]. By denoting the conventional energy drawn from the main grid to microgrid j at time slot i as $G_{j,i} \geq 0$, the energy cost at time slot i is given by

$$f_i(\{G_{j,i}\}) = \sum_{j=1}^2 \lambda_{j,i} G_{j,i}, \quad (2)$$

where $\lambda_{j,i} > 0$ is the price of purchasing one unit of power from the main grid for microgrid j at time slot i . We assume that prices $\lambda_{j,i}$, $\forall j \in \mathcal{J}$, $\forall i \in \mathcal{N}$, are known to microgrids.

3) *Load and Renewable Energy Generation*: Denote the load and renewable energy generation of microgrid j at time slot i by $L_{j,i} \geq 0$, and $RE_{j,i} \geq 0$, respectively. We assume that $L_{j,i}$'s and $RE_{j,i}$'s are predictable but with finite prediction errors, due to their randomness in practice. Suppose that the predictable load and renewable energy generation values of microgrid j at time slot i are denoted as $\bar{L}_{j,i}$ and $\bar{RE}_{j,i}$, respectively. We then have $L_{j,i} = \bar{L}_{j,i} + \delta_{j,i}^L$ and $RE_{j,i} = \bar{RE}_{j,i} + \delta_{j,i}^{RE}$, where $\delta_{j,i}^L$ and $\delta_{j,i}^{RE}$ denote the prediction errors for the load and renewable energy of microgrid j at time slot i , respectively, which are modeled by arbitrary realizations over time. We thus model the *net energy profile* in microgrid j as

$$\Delta_{j,i} = \bar{\Delta}_{j,i} + \delta_{j,i}, \quad \forall i \in \mathcal{N} \quad (3)$$

where $\bar{\Delta}_{j,i} = \bar{RE}_{j,i} - \bar{L}_{j,i}$ and $\delta_{j,i} = \delta_{j,i}^{RE} - \delta_{j,i}^L$.

4) *Power Transmission Loss*: In practical systems, power loss is inevitable over transmission lines due to the ohmic resistance. Let $E_{j,i} \geq 0$ denote the power transferred from microgrid j to microgrid \bar{j} , $\bar{j} \in \mathcal{J} \setminus \{j\}$ at time slot i . Denote $R > 0$ and $V > 0$ as the ohmic resistance of the transmission line connecting the two microgrids per length unit and its operating voltage, respectively. The transmission loss is then modeled as $P^{\text{loss}}(E_{j,i}) = \beta E_{j,i}^2$, where $\beta = (R \cdot d)/V^2$

¹In practice, there are other constraints besides (1) for ESSs such as the maximum charging/discharging rates, which can further limit their operation.

[25]. Accordingly, the net power received in microgrid \bar{j} from microgrid j at time slot i can be expressed as $E_{j,i} - \beta E_{j,i}^2$.

5) *Transmission Line Capacity*: The power transferred over the line connecting the two microgrids is constrained by the transmission line capacity, denoted by $0 \leq \bar{E} < 1/(2\beta)$, due to, e.g., thermal constraints of its conductors. Accordingly, we have the following constraints for the power transferred from microgrid j to \bar{j} as

$$0 \leq E_{j,i} \leq \bar{E}, \quad \forall i \in \mathcal{N}. \quad (4)$$

6) *Energy Neutralization Constraint*: We assume that the energy deficit in microgrid j is always satisfied by (i) discharging its ESS and/or (ii) drawing energy from the other microgrid and/or (iii) drawing conventional energy from the main grid. Accordingly, the energy neutralization constraints in microgrid j are expressed as

$$G_{j,i} + \Delta_{j,i} - C_{j,i} + D_{j,i} - E_{j,i} + E_{\bar{j},i} - \beta E_{j,i}^2 \geq 0, \quad \forall i \in \mathcal{N}. \quad (5)$$

Note that in case of energy surplus $\Delta_{j,i} > 0$, part of the energy may be curtailed due to the limited capacities of ESSs and the transmission line connecting the two microgrids. In this case, (5) will hold with a strict inequality.

With the aforementioned models, we now proceed to jointly optimize the energy drawn from the main grid $\{G_{j,i}\}$, that exchanged between microgrids $\{E_{j,i}\}$, and that charged/discharged to/from the ESSs of individual microgrids $\{C_{j,i}, D_{j,i}\}$ to minimize the total cost of the energy drawn from the main grid, i.e., $\sum_{i=1}^N f_i(\{G_{j,i}\})$, while satisfying the given constraints of ESSs, loads, and the transmission line. We thus formulate the optimization problem as³

$$\begin{aligned} \text{(P1)} : \quad & \min_{\{G_{j,i}\}, \{E_{j,i}\}, \{C_{j,i}\}, \{D_{j,i}\}} \sum_{j=1}^2 \sum_{i=1}^N \lambda_{j,i} G_{j,i} \\ \text{s.t.} \quad & (1), (4), \text{ and } (5), \quad \forall j \in \mathcal{J} \\ & G_{j,i} \geq 0, \quad C_{j,i} \geq 0, \quad D_{j,i} \geq 0, \quad \forall j \in \mathcal{J}, \quad \forall i \in \mathcal{N}. \end{aligned}$$

To solve (P1), we first assume that $\Delta_{j,i}$'s can be perfectly predicted without any error, i.e., $\delta_{j,i} = 0$, $\forall j \in \mathcal{J}$, $\forall i \in \mathcal{N}$; accordingly, we solve the off-line optimization problem. Next, we propose online algorithms for the practical setup of noisy net energy profiles with arbitrary error realizations of $\delta_{j,i}$'s.

III. OFF-LINE OPTIMIZATION AND ENERGY COOPERATION VERSUS STORAGE TRADEOFF IN COST REDUCTION

In this section, we consider the off-line optimization for (P1) by assuming $\{\Delta_{j,i}\}$ are perfectly known. It can be verified that (P1) is a convex optimization problem, which can be solved by standard convex optimization techniques such as the interior point method [26]. Alternatively, we apply the Lagrange duality method to solve this problem in order to

²Since voltages of lines connecting the main grid to microgrids are high (over 220 KV), it follows that the corresponding β 's are very small and thus we can ignore the resulting losses in these lines.

³It is worth noting that (P1) with deterministic $\Delta_{j,i}$'s can be regarded as the classical DC power flow problem that takes into account only the active power. In this case, we assume that the magnitude and phase of the voltage of the transmission line can be adjusted using independent VAR compensators, e.g., series/shunt capacitor/inductance banks [27].

draw useful insights from the solution and enable distributed implementation. Through a numerical example, we then show that the microgrids' energy cooperation can help reduce the required storage capacities of ESSs, i.e., S_j^{\max} , under the same load requirement. We also compare the impacts of microgrids' energy cooperation versus their ESSs on the total energy cost saving, which motivate our design of the online energy management algorithms later in Section IV.

A. Optimal Off-line Solution

Denote the optimal solution to (P1) as $\{G_{j,i}^*, E_{j,i}^*, C_{j,i}^*, D_{j,i}^*\}$. Based on the Lagrange duality method, the optimal solution to (P1) is given in the following proposition.

Proposition 3.1: The optimal solution to (P1) is given by

$$E_{j,i}^* = \begin{cases} 0 & \gamma_{j,i}^* = 0 \\ \min \left(\left[\frac{\gamma_{j,i}^* - \gamma_{\bar{j},i}^*}{2\gamma_{j,i}^* \beta} \right]^+, \bar{E} \right) & \text{otherwise} \end{cases}, \quad (6)$$

for $\forall j \in \mathcal{J}$, $\forall i \in \mathcal{N}$, where $[x]^+ \triangleq \max(0, x)$, and $0 \leq \gamma_{j,i}^* \leq \lambda_{j,i}$, $\forall j \in \mathcal{J}$, $\forall i \in \mathcal{N}$, are the optimal Lagrange dual variables corresponding to energy neutralization constraints given in (5). Given $\{E_{j,i}^*\}$ in (6), (P1) becomes a linear programming (LP) over $\{G_{j,i}, C_{j,i}, D_{j,i}\}$. We thus solve the following LP to obtain $\{G_{j,i}^*, C_{j,i}^*, D_{j,i}^*\}$.

$$\min_{\{G_{j,i} \geq 0\}, \{C_{j,i} \geq 0\}, \{D_{j,i} \geq 0\}} \sum_{j=1}^2 \sum_{i=1}^N \lambda_{j,i} G_{j,i}$$

s.t. (1), $\forall j \in \mathcal{J}$

$$G_{j,i} + \Delta_{j,i} - C_{j,i} + D_{j,i} - t_{j,i}^* \geq 0, \quad \forall j \in \mathcal{J}, \quad \forall i \in \mathcal{N} \quad (7)$$

where $t_{j,i}^* = E_{j,i}^* - E_{\bar{j},i}^* + \beta E_{j,i}^{*2}$.

Proof: Please refer to Appendix A. ■

The optimal solution proposed in Proposition 3.1 can be implemented in a *distributed* manner, where the central control unit computes $\{\gamma_{j,i}^*\}$ using a subgradient based method (see Appendix A for the detail), based on the information received from the two microgrids. The optimal Lagrange dual variables $\{\gamma_{j,i}^*\}$ are sent to the microgrids, each of which then independently derives $\{G_{j,i}^*, E_{j,i}^*, C_{j,i}^*, D_{j,i}^*\}$ from (6) and (7). Furthermore, given $\gamma_{j,i}^*$ and $\gamma_{\bar{j},i}^*$, it can be verified from (6) that $E_{j,i}^*$ and $E_{\bar{j},i}^*$ cannot be non-zero simultaneously at each time slot i . This result is intuitively correct, since it is not optimal for the microgrids to transfer energy at the same time due to the energy loss in the transmission line.

Remark 3.1: The Lagrange dual variable $\gamma_{j,i}$ can be interpreted as the marginal cost in microgrid j , defined as the increment in the total energy cost due to consuming extra unit power in this microgrid to satisfy its load, to charge its ESS and/or to transfer to microgrid \bar{j} . From (6), it follows that when $\gamma_{j,i} < \gamma_{\bar{j},i}$, energy flows from microgrid j to microgrid \bar{j} to reduce the total energy cost.

Last, note that for the general case of more than two microgrids, the same standard procedure can be followed to formulate and optimally solve the off-line energy management problem. For brevity, we omit the details here, while simulation results will be provided later in Section V for the online energy cooperation in the general case.

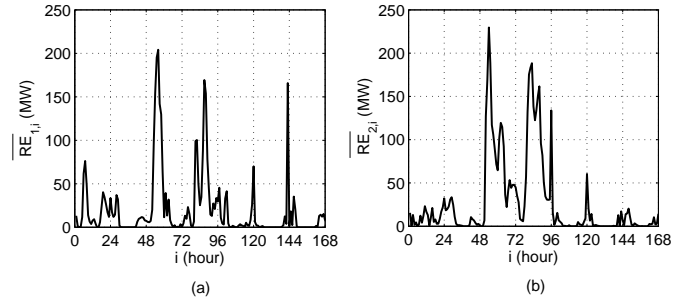


Fig. 2. Hourly predicted wind energy generation over one week for (a) microgrid 1 and (b) microgrid 2.

TABLE I
SYSTEM PARAMETERS

Energy Storage Systems		Transmission line connecting microgrids	
α_j^c	0.85	R (Peacock)	0.0945 Ω/Km
α_j^d	0.85	R (Goat)	0.2923 Ω/Km
$S_{j,1}$	0	V	33 KV
S_1^{\min}	0	d	45 Km
S_1^{\max}	80 MW	\bar{E}	40 MW
S_2^{\max}	110 MW		

B. Impact of Energy Cooperation on Energy Storage Requirement

In this subsection, we aim to show how the microgrids' energy cooperation reduces the need for ESSs with large storage capacities in the system. For the purpose of exposition, we consider a system with two microgrids that are located in Tucson, Arizona, United States [23].⁴ Microgrid 1 and microgrid 2 own 70 and 80 Vestas V90 wind turbines, respectively, where each turbine has the rated power output of 3 MW. We model the renewable energy generation in the two microgrids at each particular time slot i , i.e., $[RE_{1,i} \ RE_{2,i}]^T$, as a Gaussian random vector with mean $[\bar{RE}_{1,i} \ \bar{RE}_{2,i}]^T$, variance $[\sigma_{RE_{1,i}}^2 \ \sigma_{RE_{2,i}}^2]^T$ with $\sigma_{RE_{j,i}} > 0$, $\forall j \in \mathcal{J}$, $\forall i \in \mathcal{N}$, and the covariance matrix Σ_i given by

$$\Sigma_i = \begin{bmatrix} \sigma_{RE_{1,i}}^2 & \rho_{RE_{1,i}, RE_{2,i}} \sigma_{RE_{1,i}} \sigma_{RE_{2,i}} \\ \rho_{RE_{1,i}, RE_{2,i}} \sigma_{RE_{1,i}} \sigma_{RE_{2,i}} & \sigma_{RE_{2,i}}^2 \end{bmatrix},$$

where $\rho_{RE_{1,i}, RE_{2,i}}$ is the correlation coefficient between $RE_{1,i}$ and $RE_{2,i}$. We assume $\sigma_{RE_{j,i}} = \sigma$, $\forall j \in \mathcal{J}$, $\forall i \in \mathcal{N}$, and $\rho_{RE_{1,i}, RE_{2,i}} = \rho$, $\forall i \in \mathcal{N}$. We set the predictable renewable energy generation in the microgrids $\{\bar{RE}_{j,i}\}$ as the hourly wind energy generation over a week (from 5 August 2006 to 11 August 2006) in Tucson [23], as shown in Fig. 2. We consider time-invariant aggregate loads in microgrids with $\bar{L}_{1,i} = 20$ MW and $\bar{L}_{2,i} = 30$ MW, $\forall i \in \mathcal{N}$, and for simplicity assume that $\{L_{j,i}\}$ can be perfectly predicted, i.e., $\delta_{j,i}^L = 0$, $\forall j \in \mathcal{J}$, $\forall i \in \mathcal{N}$. Accordingly, from (3) it follows that $[\Delta_{1,i} \ \Delta_{2,i}]^T = [RE_{1,i} - 20 \ RE_{2,i} - 30]^T$, $\forall i \in \mathcal{N}$. The prediction error component in the net energy profile is also obtained as $\delta_{j,i} = \delta_{j,i}^{RE}$, $\forall j \in \mathcal{J}$, $\forall i \in \mathcal{N}$. As a result, $\sigma_{\Delta_{j,i}} = \sigma_{RE_{j,i}} = \sigma$ and $\rho_{\Delta_{1,i}, \Delta_{2,i}} = \rho_{RE_{1,i}, RE_{2,i}} = \rho$, $\forall j \in \mathcal{J}$, $\forall i \in \mathcal{N}$, where $\sigma_{\Delta_{j,i}} > 0$ and $\rho_{\Delta_{1,i}, \Delta_{2,i}}$ denote

⁴We assume that microgrid 1 comprises wind generators with site IDs: 151, 161, 162, 163, 170, 171, 189, and microgrid 2 with site IDs: 152, 172, 181, 190, 200, 216, 219, 220 [23].

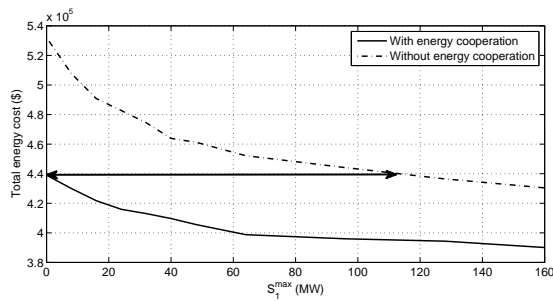


Fig. 3. Total energy cost of microgrids versus S_1^{\max} for two cases with and without energy cooperation.

the standard deviation of $\Delta_{j,i}$ and the correlation between $\Delta_{1,i}$ and $\Delta_{2,i}$, respectively. We consider the average daily electricity prices for both peak and off-peak hours in Tucson [28] and set $\lambda_{j,i} = 89.85$ \$/MW, $\forall j \in \mathcal{J}, \forall i \in \mathcal{N}$. The parameters of ESSs and the transmission line connecting the two microgrids [29] are given in Table I.

Given the aforementioned system setup and by setting $\rho = 0$ and $\sigma = 30$ MW, we plot the total energy cost versus the storage capacity in microgrid 1 in Fig. 3, while $S_2^{\max} = 110$ MW is assumed constant. It is observed that in both cases with and without energy cooperation, the total energy cost of microgrids decreases over S_1^{\max} , which is due to less waste in surplus energy. Furthermore, it is observed that microgrids with energy cooperation can achieve the total energy cost target with a smaller S_1^{\max} as compared to the case without energy cooperation. For example, as shown in Fig. 3, to achieve the total energy cost of 4.4×10^5 \$, we can set $S_1^{\max} = 0$ in the case with energy cooperation, while we need $S_1^{\max} = 115$ MW in the case without energy cooperation. This shows that microgrids' energy cooperation can significantly reduce the required storage capacities.

C. Energy Cooperation versus Storage for Cost Reduction

Although both microgrids' energy cooperation and use of ESSs can save the total energy cost, it is not clear yet under what conditions one can be more effective than the other. In this subsection, we further investigate this issue via simulations.

Under the same system setup as in Section III-B and by setting $\sigma = 30$ MW, we plot the total energy cost versus the correlation coefficient⁵ between the microgrids' net energy profiles ρ in Figs. 4-a and 4-b, for two different types of transmission line. It is observed that the combination of both microgrids' energy cooperation and ESSs yields the lowest total energy cost, while the highest total energy cost results from the absence of both energy cooperation and ESSs. When ρ is close to -1 , energy cooperation saves the total energy cost significantly, since it is more likely that the energy surplus in one microgrid compensates the energy deficit in the other one. In contrast, when ρ is close to 1, energy cooperation is less

⁵The correlation between net energy profiles in microgrids depends on various parameters such as the type of their renewable energy generators (e.g., one microgrid mainly using solar energy while the other mainly using wind energy), their geographical diversity, etc.

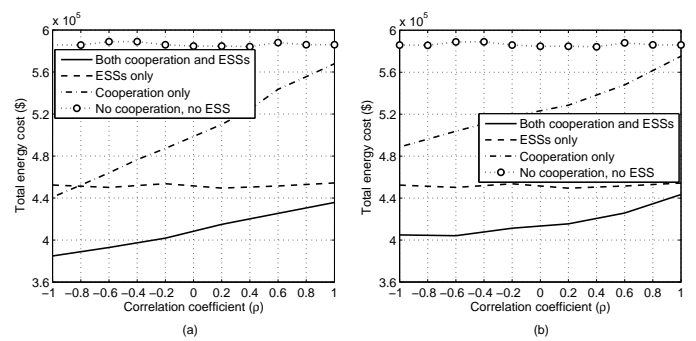


Fig. 4. Microgrids' total energy cost for different operation modes: (a) Peacock line with $R = 0.0945$ Ω/Km , (b) Goat line with $R = 0.2923$ Ω/Km .

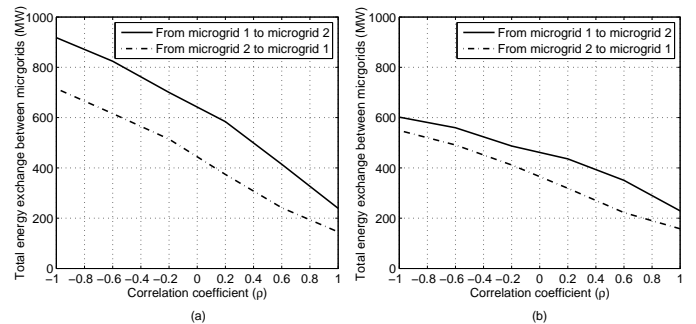


Fig. 5. Microgrids' total energy exchange: (a) Peacock line with $R = 0.0945$ Ω/Km , (b) Goat line with $R = 0.2923$ Ω/Km .

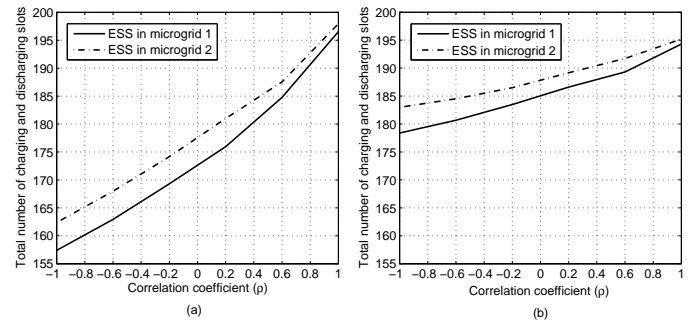


Fig. 6. Microgrids' total number of charging and discharging slots: (a) Peacock line with $R = 0.0945$ Ω/Km , (b) Goat line with $R = 0.2923$ Ω/Km .

effective, while most of cost saving is due to ESSs. Last, Fig. 4-b shows that the impact of microgrids' energy cooperation in reducing the total energy cost is less significant as compared to Fig. 4-a, when the transmission line with larger resistance ($R = 0.2923$ Ω/Km) is deployed, due to high energy loss during the energy exchange.

Figs. 5-a and 5-b show the total energy exchanged between microgrids, i.e., $\sum_{i=1}^N E_{j,i}$, $\forall j \in \mathcal{J}$, for two different types of transmission line. It is observed that the total energy exchanged between microgrids decreases over ρ due to their highly correlated net energy profiles. In this case, each microgrid relies more on its ESS to deal with energy deficit and thus the total number of times that the ESS is charged/discharged, i.e. $\sum_{i=1}^N 1\{C_{j,i} > 0\} + 1\{D_{j,i} > 0\}$ with $1\{\cdot\}$ denoting the indicator function, increases over ρ , as shown in Figs. 6-a and 6-b. It is also observed that while high resistance of the transmission line reduces the total energy exchanged between

microgrids (see Fig. 5-a and Fig. 5-b), it leads to more frequent charging/discharging of ESSs (see Fig. 6-a and Fig. 6-b).

In summary, our above results show that both the energy cooperation as well as ESSs have significant impacts on the microgrids' total energy cost reduction, while one can be more effective than the other depending on the system setup. We thus draw the following observations for both long-term and short-term plannings of cooperative microgrids system:

- For the *long-term* planning problem that is aimed to minimize the deployment cost, if the energy cost saving is mainly due to microgrids' energy cooperation, ESSs with small storage capacities should be used for the cost-effective operation of microgrids. In contrast, if microgrids' energy cooperation is not effective in reducing the total energy cost, enabling energy cooperation may not be essential, while installing ESSs with large storage capacities is more effective.
- For the *short-term* planning problem, which, on the other hand, aims to minimize the operation cost of microgrids with the ESSs and transmission line between microgrids already deployed, the above results show that the effectiveness of microgrids' energy cooperation and their ESSs in reducing the total energy cost depends on several parameters, e.g., the correlation between microgrids' net energy profiles, the resistance of the line connecting them, charging/discharging efficiency parameters of ESSs, etc. Accordingly, in the next section, we design two algorithms, which use ESSs or energy cooperation with higher priority, respectively. Based on the system setup and using practical data, the algorithm that leads to a lower total energy cost can be chosen off-line and then adopted for real-time implementation.

IV. ONLINE ALGORITHMS FOR REAL-TIME ENERGY MANAGEMENT OF MICROGRIDS

In this section, we consider the practical setup of noisy net energy profiles, i.e., $\delta_{j,i} \neq 0, \forall j \in \mathcal{J}, \forall i \in \mathcal{N}$. We aim to propose online algorithms for the real-time energy management of cooperative microgrids such that their total energy cost is minimized. By assuming the energy prices $\lambda_{j,i} = \lambda \geq 0, \forall j \in \mathcal{J}, \forall i \in \mathcal{N}$ for simplicity, we propose the following algorithms.

A. Store-Then-Cooperate

In this algorithm, the microgrid with energy surplus first charges its ESS and then transfers the remaining (if any) to the other microgrid to satisfy its energy deficit or to be stored in its ESS. This algorithm is more effective when the energy cost saving is mainly due to ESSs rather than microgrids' energy cooperation, e.g., the energy loss in the transmission line connecting the two microgrids is high. We set $\{G_{j,i}, E_{j,i}, C_{j,i}, D_{j,i}\}$ all equal to zero in the algorithm, unless otherwise stated. The algorithm is described as follows:

Case A.1) $\Delta_{1,i} \geq 0$ and $\Delta_{2,i} \geq 0$. In this case, each microgrid first charges its ESS. We thus have

$$\begin{aligned} C_{j,i} &= \min\{(S_j^{\max} - S_{j,i})/\alpha_j^c, \Delta_{j,i}\}, \quad j \in \mathcal{J} \\ S_{j,i+1} &\leftarrow S_{j,i} + \alpha_j^c C_{j,i}, \quad j \in \mathcal{J}. \end{aligned} \quad (8)$$

If $S_{1,i+1} = S_1^{\max}$ and $S_{2,i+1} = S_2^{\max}$ or $S_{1,i+1} < S_1^{\max}$ and $S_{2,i+1} < S_2^{\max}$, then this case terminates. Otherwise if $S_{2,i+1} < S_2^{\max}$ and $S_{1,i+1} = S_1^{\max}$, then microgrid 1 transfers all its energy surplus to microgrid 2 and the decision variables are updated as

$$\begin{aligned} E_{1,i} &\leftarrow \min\{\Delta_{1,i} - C_{1,i}, \bar{E}\}, \\ C_{2,i} &\leftarrow C_{2,i} + \min\{E_{1,i} - \beta E_{1,i}^2, (S_2^{\max} - S_{2,i+1})/\alpha_2^c\}, \\ S_{2,i+1} &\leftarrow S_{2,i+1} + \alpha_2^c (\min\{E_{1,i} - \beta E_{1,i}^2, (S_2^{\max} - S_{2,i+1})/\alpha_2^c\}). \end{aligned} \quad (9)$$

Similarly, if $S_{1,i+1} < S_1^{\max}$ and $S_{2,i+1} = S_2^{\max}$, then decision variables are updated as (9) with the roles of microgrids 1 and 2 swapped.

Case A.2) $\Delta_{1,i} \geq 0$ and $\Delta_{2,i} < 0$. In this case, the energy surplus in microgrid 1 is first stored in its ESS. The remaining energy (if any) is transferred to microgrid 2. The algorithm thus sets

$$\begin{aligned} C_{1,i} &= \min\{\Delta_{1,i}, (S_1^{\max} - S_{1,i})/\alpha_1^c\}, \\ E_{1,i} &= \min\{\Delta_{1,i} - C_{1,i}, \bar{E}\}, \\ S_{1,i+1} &\leftarrow S_{1,i} + \alpha_1^c C_{1,i}. \end{aligned} \quad (10)$$

Let $\Delta'_{2,i} = \Delta_{2,i} + E_{1,i} - \beta E_{1,i}^2$. If $\Delta'_{2,i} \geq 0$, the transferred energy from microgrid 1 compensates the energy deficit in microgrid 2. The remaining energy (if any) is stored in the ESS of microgrid 2, i.e.,

$$\begin{aligned} C_{2,i} &= \min\{\Delta'_{2,i}, (S_2^{\max} - S_{2,i})/\alpha_2^c\}, \\ S_{2,i+1} &\leftarrow S_{2,i} + \alpha_2^c C_{2,i}. \end{aligned} \quad (11)$$

Otherwise, If $\Delta'_{2,i} < 0$, then the ESS in microgrid 2 is discharged first and the remaining energy deficit (if any) is then drawn from the main grid. We thus have

$$\begin{aligned} D_{2,i} &= \min\{\alpha_2^d S_{2,i}, -\Delta'_{2,i}\}, \quad G_{2,i} = -\Delta'_{2,i} - D_{2,i}, \\ S_{2,i+1} &\leftarrow S_{2,i} - 1/\alpha_2^d D_{2,i}. \end{aligned} \quad (12)$$

Case A.3) $\Delta_{1,i} < 0$ and $\Delta_{2,i} \geq 0$. This case is symmetric to Case A.2, with the roles of microgrid 1 and microgrid 2 swapped. We thus omit the description of the algorithm here.

Case A.4) $\Delta_{1,i} < 0$ and $\Delta_{2,i} < 0$. In this case, microgrids do not exchange energy since neither of them has energy surplus. In particular, each microgrid compensates its deficit by first discharging its ESS. The remaining energy deficit is drawn from the main grid. We thus have

$$\begin{aligned} D_{j,i} &= \min\{\alpha_j^d S_{j,i}, -\Delta_{j,i}\}, \quad G_{j,i} = -\Delta_{j,i} - D_{j,i}, \quad \forall j \in \mathcal{J} \\ S_{j,i+1} &\leftarrow S_{j,i} - 1/\alpha_j^d D_{j,i}, \quad \forall j \in \mathcal{J}. \end{aligned} \quad (13)$$

B. Cooperate-Then-Store

This algorithm is devised such that the microgrid with energy surplus first transfers energy to the other microgrid (if it has energy deficit) and stores the remaining (if any) in its ESS. This algorithm is more effective when the energy cost saving is mainly attributed to microgrids' energy cooperation rather than ESSs, e.g., the correlation between the microgrids' net energy profiles is small and the energy loss in the transmission line is low. We set $\{G_{j,i}, E_{j,i}, C_{j,i}, D_{j,i}\}$ all equal to zero in the

algorithm, unless otherwise stated. Similar to the store-then-cooperate algorithm, this algorithm is described as follows:

Case B.1) $\Delta_{1,i} \geq 0$ and $\Delta_{2,i} \geq 0$. In this case, the algorithm performs the same as Case A.1 in Section IV-A.

Case B.2) $\Delta_{1,i} \geq 0$ and $\Delta_{2,i} \leq 0$. In this case, microgrid 1 with excess energy first transfers energy to microgrid 2 with energy deficit. If the energy deficit in microgrid 2 is higher than the maximum energy that can be received from microgrid 1, i.e., $-\Delta_{2,i} \geq \bar{E} - \beta \bar{E}^2$, then we set

$$\begin{aligned} E_{1,i} &= \min\{\Delta_{1,i}, \bar{E}\}, \\ D_{2,i} &= \min\{-\Delta_{2,i} + E_{1,i} - \beta E_{1,i}^2, \alpha_2^d S_{2,i}\}, \\ G_{2,i} &= -(\Delta_{2,i} + E_{1,i} - \beta E_{1,i}^2) - D_{2,i}, \\ S_{1,i+1} &\leftarrow S_{1,i}, \quad S_{2,i+1} \leftarrow S_{2,i} - 1/\alpha_2^d D_{2,i}. \end{aligned} \quad (14)$$

Otherwise, if $-\Delta_{2,i} < \bar{E} - \beta \bar{E}^2$, then microgrid 1 transfers energy as much as is needed in microgrid 2. Thus, we have

$$E_{1,i} = \min\{\Delta_{1,i}, (1 - \sqrt{1 + 4\beta\Delta_{2,i}})/(2\beta)\}. \quad (15)$$

Define $\Delta'_{2,i} = \Delta_{2,i} + E_{1,i} - \beta E_{1,i}^2$. If $\Delta'_{2,i} \leq 0$, then the remaining energy deficit in microgrid 2 is compensated using its ESS and the main grid, and $\{G_{2,i}, D_{2,i}\}$ are derived from (14). Otherwise, if $\Delta'_{2,i} > 0$, then the energy surplus in microgrid 1 is first stored in its ESS and the remaining energy (if any) is sent to microgrid 2 and stored in its ESS. The algorithm thus sets

$$\begin{aligned} C_{1,i} &= \min\{\Delta_{1,i} - E_{1,i}, (S_1^{\max} - S_{1,i})/\alpha_1^c\}, \\ E_{1,i} &\leftarrow E_{1,i} + \min\{\Delta_{1,i} - E_{1,i} - C_{1,i}, \bar{E} - E_{1,i}\}, \\ C_{2,i} &= \min\{E_{1,i} + \Delta_{2,i} - \beta E_{1,i}^2, (S_2^{\max} - S_{2,i})/\alpha_2^c\}, \\ S_{1,i+1} &\leftarrow S_{1,i} + \alpha_1^c C_{1,i}, \quad S_{2,i+1} \leftarrow S_{2,i} + \alpha_2^c C_{2,i}. \end{aligned} \quad (16)$$

Case B.3) $\Delta_{1,i} \leq 0$ and $\Delta_{2,i} \geq 0$. This case is symmetric to Case B.2, with the roles of microgrid 1 and microgrid 2 swapped. We thus omit the description of the algorithm here.

Case B.4) $\Delta_{1,i} \leq 0$ and $\Delta_{2,i} \leq 0$. In this case, the algorithm performs the same as Case A.4 in Section IV-A.

In practice, given the system setup and based on the historical data, we can select one of the above two algorithms which results in a lower energy cost by off-line computation and then implement it for microgrids' real-time energy management. It is worth noting that every single decision made at each time slot may not be optimal in the above approach; however, the overall performance of the selected algorithm is optimized, since the off-line optimization has taken into account all impacts of ESS capacities, transmission loss, predicted renewable energy generations and loads, etc.

C. Performance Evaluation

First, we compare the performance of our proposed online algorithms using the same system setup in Section III-B. Fig. 7 and Fig. 8 show the total energy cost of microgrids versus the prediction error variance σ^2 , for the two different types of transmission line. It is observed from Fig. 7 that the cooperate-then-store online algorithm performs closer to the optimal solution derived from the off-line optimization, while the store-then-cooperate algorithm performs better in Fig. 8.

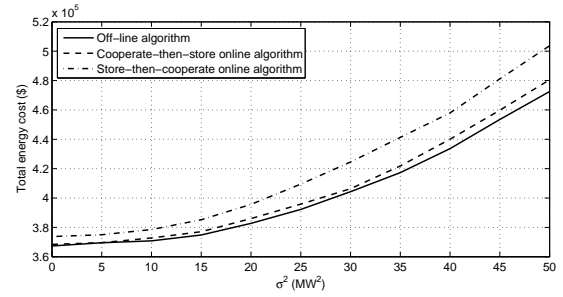


Fig. 7. Performance comparison of online algorithms when $\rho = 0$ and $R = 0.0945 \Omega/\text{Km}$.

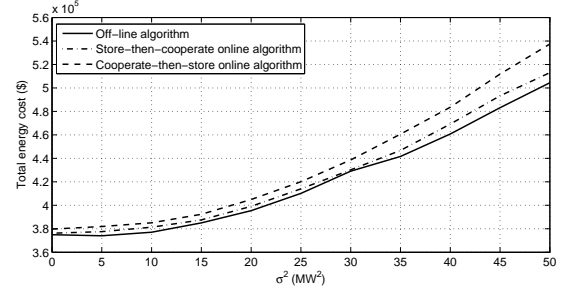


Fig. 8. Performance comparison of online algorithms when $\rho = 0$ and $R = 0.2923 \Omega/\text{Km}$.

This is because the resistance of the transmission line in Fig. 7 is lower than that in Fig. 8; hence, energy cooperation is more effective in reducing the total energy cost in Fig. 7.

Next, we consider the special setup where both microgrids have mainly wind/solar energy generators. In this case, it can be shown that the correlation coefficient between microgrids' renewable energy generations $\rho_{RE_{1,i}, RE_{2,i}}$ is distance-dependent and can be approximated by an exponential function of the distance between microgrids, d , as follows [30].

$$\rho_{RE_{1,i}, RE_{2,i}} = e^{-ad^b}, \quad \forall i \in \mathcal{N} \quad (17)$$

where a and b are empirically obtained coefficients by e.g. curve fitting techniques. Denote the prediction error variance of $L_{j,i}$ as $\sigma_{L_{j,i}}^2$. We then have the following proposition.

Proposition 4.1: By assuming that $L_{1,i}$ and $L_{2,i}$, as well as $L_{j,i}$ and $RE_{k,i}$, $\forall j, k \in \mathcal{J}, \forall i \in \mathcal{N}$ are independent random variables, it can be shown that for $\forall i \in \mathcal{N}$, we have

$$\rho_{\Delta_{1,i}, \Delta_{2,i}} = \frac{\sigma_{RE_{1,i}} \sigma_{RE_{2,i}}}{\sqrt{\sigma_{RE_{1,i}}^2 + \sigma_{L_{1,i}}^2} \sqrt{\sigma_{RE_{2,i}}^2 + \sigma_{L_{2,i}}^2}} \rho_{RE_{1,i}, RE_{2,i}}. \quad (18)$$

Proof: Please refer to Appendix B. ■

We use the same system setup as in Section III-B. Due to our assumption that $\delta_{j,i}^L = 0$, we have $\sigma_{L_{j,i}} = 0$, $\forall j \in \mathcal{J}, \forall i \in \mathcal{N}$. Accordingly, it follows from (18) that $\rho_{\Delta_{1,i}, \Delta_{2,i}} = \rho_{RE_{1,i}, RE_{2,i}} = \rho$, $\forall i \in \mathcal{N}$, which can be computed from (17) with given distance d . We also set $a = 0.04$ and $b = 0.95$. Next, we plot the energy cost saving versus the distance between the two microgrids d for both types of transmission line in Fig. 9. It is observed that the maximum energy cost saving occurs at a distance threshold denoted by \bar{d} . The distance threshold in Goat (higher ohmic

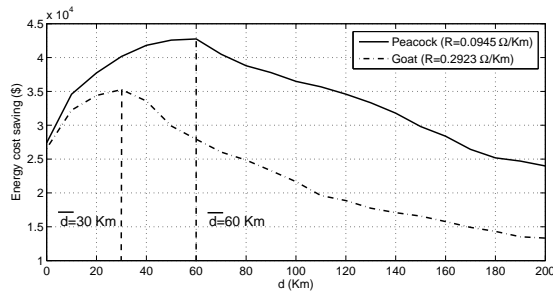


Fig. 9. Energy cost saving versus distance d .

resistance) is $\bar{d} = 30$ Km which is smaller than that in Peacock (lower ohmic resistance) with $\bar{d} = 60$ Km. This result is expected, since the transmission loss per Km in Goat is higher than that in Peacock; hence, the effectiveness of energy cooperation is reduced given the same distance. Last, it is observed that the energy cost saving increases for $0 \leq d \leq \bar{d}$, while the opposite is true for $d \geq \bar{d}$. For $0 \leq d \leq \bar{d}$, the correlation between net energy profiles in the two microgrids reduces considerably as d increases and thus results in more energy exchange, while the increase in the transmission loss is relatively lower. Thus, the energy cost saving increases with d . However, for $d \geq \bar{d}$, the decrease in the energy cost saving caused by the relatively high transmission loss is dominated by the energy cooperation gain due to more independent net energy profiles. From these observations, we can conclude that microgrids' energy cooperation is more effective when $0 \leq d \leq \bar{d}$ and cooperate-then-store algorithm is thus more suitable for the online energy management in this case. In contrast, when $d \geq \bar{d}$, the transmission loss is large such that the effectiveness of energy cooperation becomes diminished; as a result, store-then-cooperate algorithm performs better in this case.

V. EXTENSION TO MORE THAN TWO MICROGRIDS

In this section, we extend our proposed online algorithms in Section IV to the general case of more than two microgrids. For the purpose of illustration, we consider a power system consisting of four microgrids, each of which is modeled based on the real data available from California, US, over a one-week scheduling period (from 1 January, 2006 to 7 January, 2006) [23], [31]–[33]. The result can be also applied for arbitrary even number of microgrids. We model energy consumers in the microgrid based on the available data of actual residential and commercial users given in [31]. The number of energy consumers in each microgrid and their types are given in Table II. The solar and wind energy generation data are based on [23], [32]. The number of wind and solar PV stations in each microgrid is given in Table III. We also consider sodium-sulfur based batteries for ESSs in microgrids and set their charging and discharging efficiencies as $\alpha_j^c = \alpha_j^d = 0.87$, $\forall j \in \{1, \dots, 4\}$ [34]. The total ESS capacities in microgrids are presented in Table IV. For simplicity, we assume microgrids are connected to each other via the same type of transmission lines, i.e. Peacock, with $R = 0.0945 \Omega/\text{Km}$ and set $V = 33$ KV. By denoting the distance between microgrid j and microgrid k as d_{jk} (or d_{kj}), $j, k \in \{1, \dots, 4\}$, $j \neq k$, the

TABLE II
NUMBER OF LOADS IN MICROGRIDS

Microgrid index	No. of Commercial loads	No. of residential loads
1	390	9500
2	450	12000
3	100	5000
4	250	8000

TABLE III
RENEWABLE ENERGY GENERATION IN MICROGRIDS

Microgrid index	No. of wind stations	No. of solar PV stations
1	2	5
2	5	2
3	0	8
4	4	0

TABLE IV
ESS CAPACITIES IN MICROGRIDS

Microgrid index	Total ESS capacity (MW)
1	80
2	110
3	80
4	110

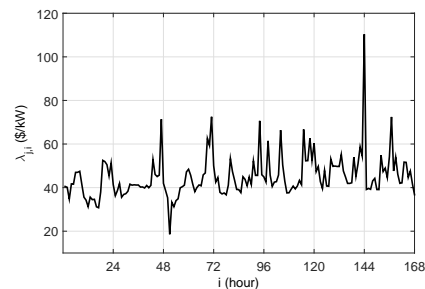


Fig. 10. Hourly market electricity price from CAISO [33].

distances between microgrids are set as $d_{12} = 18$, $d_{13} = 40$, $d_{14} = 46$, $d_{23} = 55$, $d_{24} = 45$, and $d_{34} = 34$ Km. The electricity prices offered by the main grid to all microgrids are assumed equal and set according to CAISO electricity market [33], as shown in Fig. 10.

For the case that renewable energy generation and load are perfectly known to all microgrids, we can solve the off-line optimization using the Lagrange duality method, following the same procedure given in Proposition 3.1. While for the practical setup of unknown renewable energy generation/load with prediction errors, we propose a *clustering* based algorithm, where the algorithm first divides microgrids into two groups each consisting of two microgrids, and assumes that only microgrids within the same group can have energy cooperation with each other. Next, store-then-cooperate/cooperate-then-store online algorithms proposed in Section III-C are used for real-time energy management in each group.

In practice, various methods can be adopted to group microgrids. Particularly, from the results shown in Section III-C on the effectiveness of energy cooperation on reducing microgrids' total energy cost, we know that the distance between microgrids and the correlation coefficient between their net energy profiles can significantly affect the performance gain of energy cooperation. Accordingly, one possible

TABLE V
MICROGRIDS' ENERGY COSTS IN DIFFERENT CLUSTERING CASES

Microgrids clustering	Total energy costs of microgrids (\$)
Case I: 1 and 2, 3 and 4	4.7547×10^5
Case II: 1 and 3, 2 and 4	4.7902×10^5
Case III: 1 and 4, 2 and 3	5.1335×10^5

TABLE VI
PERFORMANCE EVALUATION OF THE PROPOSED ONLINE ALGORITHMS
FOR THE BEST CLUSTERING CASE: CASE I

Renewable energy prediction error (%)	Off-line (\$)	Online	Performance loss (%)
15	4.836×10^5	5.0673×10^5	4.78
30	4.9043×10^5	5.20590×10^5	6.14

clustering approach can be grouping microgrids based on their distance such that those located close to each other are clustered in one group. Another approach is to group microgrids with less correlated net energy profiles (e.g., one microgrid with solar energy integration while the other one with wind energy integration). Herein, we consider a more general framework to group microgrids by making use of the off-line optimization. Specifically, we first consider all possible cases for clustering microgrids into groups of two (see Table V for three possible cases to cluster four microgrids), and solve the off-line optimization problem for each case given the system setup and the predicted values of renewable energy generation/load. Next, we choose the case resulting in the lowest total energy cost among all possible groupings. In general, the off-line optimization based clustering approach is more precise than the distance or correlation based criteria for grouping microgrids, since it considers the overall effects of distance, correlation coefficient between microgrids' net energy profiles, ESS capacities, etc.

Total energy costs obtained from the off-line optimization for the three cases of microgrids grouping are presented in Table V. It is observed that Case I, in which microgrids 1 and 2 are in one group while microgrids 3 and 4 are in the other group yields the lowest total energy cost. Given this grouping, we solve the online energy management problem using our proposed algorithms in Section IV, where the total energy costs of microgrids for 15% and 30% of renewable energy prediction errors are presented in Table VI. It is observed that our proposed online algorithms perform fairly close to the optimal off-line solution with performance loss of only 4.78% and 6.14% in the noisy environment with 15% and 30% renewable energy prediction errors, respectively. Note that in our proposed clustering based online algorithm, each microgrid can exchange energy with only one other microgrid within the same cluster and the clustering of the microgrids also remains unchanged throughout the scheduling time. However, the performance may be further improved if we devise more complex algorithms that enable simultaneous energy exchange among more than two microgrids at each time slot. In addition, clustering microgrids dynamically over time based on their instantaneous renewable energy supply and load demand may also help improve the performance of our

proposed clustering algorithm for energy cooperation.

VI. CONCLUSION

In this paper, we study the energy management problem for two cooperative microgrids. First, through the off-line optimization, we show that both microgrids' energy cooperation and use of ESSs can help mitigate the intermittent renewable energy generations and thereby reduce the total energy cost, while their effectiveness depend on several parameters such as the correlation between the microgrids' net energy profiles, the resistance of the line connecting them, etc. Based on the off-line optimization solution, we propose two online algorithms of low complexity for the real-time energy management of cooperative microgrids with arbitrary net energy profile realizations. We also propose one possible method to extend the online energy cooperation to the general case of more than two microgrids based on a clustering approach. The simulation results show that our proposed algorithms perform close to the optimal off-line solution under various practical settings.

APPENDIX A

PROOF OF PROPOSITION 3.1

Problem (P1) cannot be solved for each microgrid independently since it is not separable over decision variables $\{G_{1,i}, E_{1,i}, C_{1,i}, D_{1,i}\}$ and $\{G_{2,i}, E_{2,i}, C_{2,i}, D_{2,i}\}$ due to coupling constraints in (5). Let $\gamma_{j,i} \geq 0, \forall j \in \mathcal{J}, \forall i \in \mathcal{N}$, be the Lagrange dual variables corresponding to constraints in (5). The Lagrangian of (P1) is thus expressed as

$$\begin{aligned} \mathcal{L} = & \sum_{j=1}^2 \sum_{i=1}^N (\lambda_{j,i} - \gamma_{j,i}) G_{j,i} + \sum_{j=1}^2 \sum_{i=1}^N \gamma_{j,i} (C_{j,i} - D_{j,i}) \\ & + \sum_{j=1}^2 \sum_{i=1}^N \left(\gamma_{j,i} \beta E_{j,i}^2 + E_{j,i} (\gamma_{j,i} - \lambda_{j,i}) \right) - \sum_{j=1}^2 \sum_{i=1}^N \gamma_{j,i} \Delta_{j,i}. \end{aligned} \quad (19)$$

Accordingly, the dual function is given by

$$g(\{\gamma_{j,i}\}) = \min_{\{G_{j,i} \geq 0, \{E_{j,i} \geq 0, \{C_{j,i} \geq 0, \{D_{j,i} \geq 0\}} \}} \mathcal{L} \quad \text{s.t. (1), and (4)}. \quad (20)$$

Thus, the dual problem of (P1) is given by

$$(D1): \max_{\{\gamma_{j,i} \geq 0\}} g(\{\gamma_{j,i}\}). \quad (21)$$

Since (P1) is convex and satisfies the Slater's condition, strong duality holds between (P1) and its dual problem (D1) [26]. Hence, we can solve (P1) optimally by solving its dual problem (D1) equivalently. In the following, we first solve (20) to obtain $g(\{\gamma_{j,i}\})$ with given $\gamma_{j,i} \geq 0, \forall j \in \mathcal{J}, \forall i \in \mathcal{N}$, and then search over $\{\gamma_{j,i}\}$ to maximize $g(\{\gamma_{j,i}\})$ in (21).

We first have the following lemma.

Lemma A.1: In order for $g(\{\gamma_{j,i}\})$ to be bounded from below, it must hold that $\gamma_{j,i} \leq \lambda_{j,i}, \forall j \in \mathcal{J}, \forall i \in \mathcal{N}$.

Proof: Suppose that $\gamma_{j',i'} > \lambda_{j',i'}$ holds for some $j' \in \mathcal{J}$ and $i' \in \mathcal{N}$. In this case, by letting $G_{j',i'} \rightarrow \infty$ it can be shown from (19) and (20) that $\mathcal{L} \rightarrow -\infty$ and thus resulting $g(\{\gamma_{j,i}\})$ to become unbounded from below. Hence, $\gamma_{j,i} > \lambda_{j,i}$ cannot be true for $g(\{\gamma_{j,i}\})$ to be bounded from below. ■

From Lemma A.1, we need to solve the problem in (20) with given $\{\gamma_{j,i}\}$ satisfying $0 \leq \gamma_{j,i} \leq \lambda_{j,i}$, $\forall j \in \mathcal{J}$, $\forall i \in \mathcal{N}$. It can be readily verified that the minimization problem in (20) is now separable over $\{G_{1,i}, E_{1,i}, C_{1,i}, D_{1,i}\}$ and $\{G_{2,i}, E_{2,i}, C_{2,i}, D_{2,i}\}$, which means that it can be decomposed into two subproblems (one for each microgrid). The subproblem corresponding to microgrid j is given as follows:

$$\begin{aligned} \min_{\{G_{j,i}, E_{j,i}, C_{j,i}, D_{j,i}\}} & \sum_{i=1}^N \left((\lambda_{j,i} - \gamma_{j,i})G_{j,i} + \gamma_{j,i}(C_{j,i} - D_{j,i}) \right. \\ & \left. + \gamma_{\bar{j},i}\beta E_{j,i}^2 + E_{j,i}(\gamma_{j,i} - \gamma_{\bar{j},i}) \right) \\ \text{s.t.} & \text{(1), and (4),} \\ & G_{j,i} \geq 0, C_{j,i} \geq 0, D_{j,i} \geq 0, \forall i \in \mathcal{N}. \end{aligned} \quad (22)$$

The optimization problem in (22) can be further decomposed over $\{G_{j,i}\}$, $\{E_{j,i}\}$, and $\{C_{j,i}, D_{j,i}\}$ as follows:

$$\min_{\{G_{j,i} \geq 0\}} \sum_{i=1}^N (\lambda_{j,i} - \gamma_{j,i})G_{j,i}, \quad j \in \mathcal{J}, \quad (23)$$

$$\min_{\{0 \leq E_{j,i} \leq \bar{E}\}} \sum_{i=1}^N \gamma_{\bar{j},i}\beta E_{j,i}^2 + E_{j,i}(\gamma_{j,i} - \gamma_{\bar{j},i}), \quad j \in \mathcal{J}, \quad (24)$$

$$\begin{aligned} \min_{\{C_{j,i} \geq 0\}, \{D_{j,i} \geq 0\}} & \sum_{i=1}^N \gamma_{j,i}(C_{j,i} - D_{j,i}) \\ \text{s.t.} & \text{(1), } j \in \mathcal{J}. \end{aligned} \quad (25)$$

Given Lemma A.1, the optimal solution to (23) is given by⁶

$$G_{j,i}^* = 0, \quad j \in \mathcal{J}, \quad \forall i \in \mathcal{N}. \quad (26)$$

It can be also shown that $\{E_{j,i}^*\}$, given in the following, satisfies the Karash-Kuhn-Tucker (KKT) conditions [26] for the problem in (24) and is thus an optimal solution to (24).

$$E_{j,i}^* = \begin{cases} 0 & \gamma_{\bar{j},i} = 0 \\ \min \left(\left[\frac{\gamma_{\bar{j},i} - \gamma_{j,i}}{2\gamma_{j,i}\beta} \right]^+, \bar{E} \right) & \text{otherwise} \end{cases}, \quad (27)$$

for $j \in \mathcal{J}$, $\forall i \in \mathcal{N}$, where $[x]^+ \triangleq \max(0, x)$. The optimization problem in (25) is an LP since the objective and all constraint functions are linear. As a result, the optimal solution $\{C_{j,i}^*, D_{j,i}^*\}$ is derived by solving the following LP.

$$\{C_{j,i}^*, D_{j,i}^*\}_{i=1}^N \in \arg \min_{\substack{\{C_{j,i} \geq 0\}, \{D_{j,i} \geq 0\} \\ \text{s.t. (1)}}} \sum_{i=1}^N \gamma_{j,i}(C_{j,i} - D_{j,i}), \quad (28)$$

Given $\{G_{j,i}^*, E_{j,i}^*, C_{j,i}^*, D_{j,i}^*\}$ in (26)-(28), we obtain $g(\{\gamma_{j,i}\})$ with given $\{\gamma_{j,i}\}$ satisfying $0 \leq \gamma_{j,i} \leq \lambda_{j,i}$, $j \in \mathcal{J}$, $\forall i \in \mathcal{N}$. Next, we maximize $g(\{\gamma_{j,i}\})$ over $\{\gamma_{j,i}\}$ to solve the dual problem (D1) given in (21). Problem (D1) is concave but is not necessarily differentiable; therefore, a subgradient based method such as the ellipsoid method [35] is applied. It can be verified that subgradients of $g(\{\gamma_{j,i}\})$ are expressed as $-(\Delta_{j,i} + D_{j,i}^* - C_{j,i}^* - E_{j,i}^* + E_{\bar{j},i}^* - \beta E_{\bar{j},i}^{*2})$ at $\gamma_{j,i}$, $\forall j \in \mathcal{J}$,

⁶Note that if $\lambda_{j,i} - \gamma_{j,i} = 0$, then the optimal solution $G_{j,i}^*$ in (23) is not unique and can take any non-negative value. In this case, for simplicity, we set $G_{j,i}^* = 0$ as the optimal solution to this subproblem.

$\forall i \in \mathcal{N}$. Therefore, the optimal solution to (D1) is obtained as $\{\gamma_{j,i}^*\}$ using the ellipsoid method.

By denoting the optimal solution to (P1) as $\{G_{j,i}^*, E_{j,i}^*, C_{j,i}^*, D_{j,i}^*\}$, it can be verified that $\{E_{j,i}^*\}$ can be derived from (27) given $\{\gamma_{j,i}^*\}$. However, $\{G_{j,i}^*\}$ and $\{C_{j,i}^*, D_{j,i}^*\}$ cannot be obtained from (26) and (28) directly with given $\{\gamma_{j,i}^*\}$, since the solution to the problem in (20) is generally not unique for $\{G_{j,i}^*\}$ if $\lambda_{j,i} - \gamma_{j,i} = 0$ and/or for $\{C_{j,i}^*, D_{j,i}^*\}$ if $\gamma_{j,i} = 0$. Given $\{E_{j,i}^*\}$, (P1) becomes an LP over $\{G_{j,i}, C_{j,i}, D_{j,i}\}$, as expressed in (7), and can be easily solved via existing software such as CVX [36]. Note that given $\{\gamma_{j,i}^*\}$, each microgrid j independently computes $\{G_{j,i}^*, E_{j,i}^*, C_{j,i}^*, D_{j,i}^*\}$, which shows that the above algorithm for solving (P1) can be implemented in a distributed manner. This proposition is thus proved.

APPENDIX B

PROOF OF PROPOSITION 4.1

The correlation coefficient between $\Delta_{1,i}$ and $\Delta_{2,i}$, denoted by $\rho_{\Delta_{1,i}, \Delta_{2,i}}$, is defined as

$$\rho_{\Delta_{1,i}, \Delta_{2,i}} = \frac{\mathbb{E}[(\Delta_{1,i} - \bar{\Delta}_{1,i})(\Delta_{2,i} - \bar{\Delta}_{2,i})]}{\sigma_{\Delta_{1,i}} \sigma_{\Delta_{2,i}}}, \quad (29)$$

where $\bar{\Delta}_{j,i}$ and $\sigma_{\Delta_{j,i}}$ denote the mean and standard deviation of $\Delta_{j,i}$, respectively, and $\mathbb{E}[\cdot]$ denotes the expectation over $\Delta_{j,i}$. Due to our assumption that $L_{1,i}$ and $L_{2,i}$, as well as $L_{j,i}$ and $RE_{k,i}$, $\forall j, k \in \mathcal{J}$, $\forall i \in \mathcal{N}$, are independent random variables, it follows that $\mathbb{E}[RE_{k,i}L_{j,i}] = \mathbb{E}[RE_{k,i}]\mathbb{E}[L_{j,i}]$, $\mathbb{E}[L_{1,i}L_{2,i}] = \mathbb{E}[L_{1,i}]\mathbb{E}[L_{2,i}]$, and $\sigma_{\Delta_{j,i}}^2 = \sigma_{RE_{j,i}}^2 + \sigma_{L_{j,i}}^2$, $\forall j \in \mathcal{J}$, $\forall i \in \mathcal{N}$. Accordingly, it can be verified that $\mathbb{E}[(\Delta_{1,i} - \bar{\Delta}_{1,i})(\Delta_{2,i} - \bar{\Delta}_{2,i})] = \mathbb{E}[(RE_{1,i} - \bar{RE}_{1,i})(RE_{2,i} - \bar{RE}_{2,i})]$. Using the obtained results, it can be verified that (18) follows from (29). The proof of Proposition 4.1 is thus completed.

REFERENCES

- [1] N. Hatziargyriou, H. Asano, R. Iravani, and C. Marnay, "Microgrids," *IEEE Power & Energy Mag.*, vol. 5, no. 4, pp. 78-94, Aug. 2007.
- [2] P. Denholm, E. Ela, B. Kirby, and M. Milligan, "The role of energy storage with renewable electricity generation," *National Renewable Energy Laboratory*, Technical Report, Jan. 2010.
- [3] M. Kintner-Meyer, et al., "National assessment of energy storage for grid balancing and arbitrage: Phase 1, WECC," *Pacific Northwest National Laboratory*, June 2012.
- [4] W. Saad, Z. Han, H. V. Poor, and T. Basar, "Game-theoretic methods for the smart grid," *IEEE Signal Process. Mag.*, vol. 29, no. 5, pp. 86-105, Sep. 2012.
- [5] K. Rahbar, J. Xu, and R. Zhang, "Real-time energy storage management for renewable integration in microgrids: an off-line optimization approach," *IEEE Trans. Smart Grid*, vol. 6, no. 1, pp. 124-134, Jan. 2015.
- [6] S. Sun, M. Dong, and B. Liang, "Joint supply, demand, and energy storage management towards microgrid cost minimization," in *Proc. IEEE SmartGridComm*, pp. 109-114, Nov. 2014.
- [7] I. Koutsopoulos, V. Hatzi, and L. Tassiulas, "Optimal energy storage control policies for the smart power grid," in *Proc. IEEE SmartGridComm*, pp. 475-480, Oct. 2011.
- [8] K. Rahbar, R. Zhang, and C. C. Chai, "Privacy constrained energy management for self-interested microgrids," in *Proc. IEEE International Conference on Acoustics, Speech, and Signal Processing (ICASSP)*, pp. 3172-3176, Apr. 2015.
- [9] I. Atzeni, L. G. Ordez, G. Scutari, D. P. Palomar, and J. R. Fonollosa, "Noncooperative and cooperative optimization of distributed energy generation and storage in the demand-side of the smart grid," *IEEE Trans. Signal Process.*, vol. 61, no. 10, pp. 2454-2472, May 2013.

- [10] J. Matamoros, D. Gregoratti, and M. Dohler, "Microgrids energy trading in islanding mode," in *Proc. IEEE SmartGridComm*, pp. 49-54, Nov. 2012.
- [11] T. Cui, Y. Wang, S. Nazarian, and M. Pedram, "An electricity trade model for microgrid communities in smart grid," in *Proc. IEEE PES Innovative Smart Grid Technologies Conference (ISGT)*, pp. 1-5, Feb. 2014.
- [12] A. Ouammi, H. Dagdougui, and R. Sacile, "Optimal control of power flows and energy local storages in a network of microgrids modeled as a system of systems," *IEEE Trans. Control Sys. Tech.*, vol. 23, no. 1, pp. 128-138, Jan. 2015.
- [13] R. Minciardi and R. Sacile, "Optimal control in a cooperative network of smart power grids," *IEEE Sys. Journal*, vol. 6, no. 1, pp. 126-133, Mar. 2012.
- [14] F. Shahnia, S. Bourbour, and A. Ghosh, "Coupling neighboring microgrids for overload management based on dynamic multicriteria decision-making," *IEEE Trans. Smart Grid*, Early access.
- [15] M. Fathi and H. Bevrani, "Adaptive energy consumption scheduling for connected microgrids under demand uncertainty," *IEEE Trans. Power Delivery*, vol. 28, no. 3, pp. 1576-1583, July 2013.
- [16] D. T. Nguyen and L. B. Le, "Optimal energy management for cooperative microgrids with renewable energy resources," in *Proc. IEEE SmartGridComm*, pp. 678-683, Oct. 2013.
- [17] Z. Wang, B. Chen, J. Wang, M. M. Begovic, and C. Chen, "Coordinated energy management of networked microgrids in distribution systems," *IEEE Trans. Smart Grid*, vol. 6, no. 1, pp. 45-53, Jan. 2015.
- [18] D. Wang, X. Guan, J. Wu, P. Li, P. Zan, and H. Xu, "Integrated energy exchange scheduling for multimicrogrid system with electric vehicles," *IEEE Trans. Smart Grid*, Early access.
- [19] J. Wu and X. Guan, "Coordinated multi-microgrids optimal control algorithm for smart distribution management system," *IEEE Trans. Smart Grid*, vol. 4, no. 4, pp. 2174-2181, Dec. 2013.
- [20] H. S. V. S. K. Nunna and S. Doolla, "Demand response in smart distribution system with multiple microgrids," *IEEE Trans. Smart Grid*, vol. 3, no. 4, pp. 1641-1649, Dec. 2012.
- [21] Z. Wang, B. Chen, J. Wang, and J. Kim, "Decentralized energy management system for networked microgrids in grid-connected and islanded modes," *IEEE Trans. Smart Grid*, vol. 7, no. 2, pp. 1097-1105, Mar. 2016.
- [22] Y. K. Chia, S. Sun, and R. Zhang, "Energy cooperation in cellular networks with renewable powered base stations," *IEEE Trans. Wireless Commun.*, vol. 13, no. 12, pp. 6996-7010, December, 2014.
- [23] National Renewable Energy Laboratory, "Data & resources: western wind dataset," available online at http://www.nrel.gov/electricity/transmission/western_wind_disclaimer.html
- [24] K. Rahbar, C. C. Chai, and R. Zhang, "Real-time energy management for cooperative microgrids with renewable energy integration," in *Proc. IEEE SmartGridComm*, pp. 25-30, Nov. 2014.
- [25] A. J. Wood and B. F. Wollenberg, *Power Generation, Operation, and Control*, Wiley, 1996.
- [26] S. Boyd and L. Vandenberghe, *Convex Optimization*, Cambridge University Press, 2004.
- [27] G. Kasal and B. Singh, "Decoupled voltage and frequency controller for isolated asynchronous generators feeding three-phase four-wire loads," *IEEE Trans. Power Delivery*, vol. 23, no. 2, pp. 966-973, Apr. 2008.
- [28] Tucson Electric Power, "Customer care: rates, Residential Time-of-Use," available online at <https://www.tep.com/customer/rates/>
- [29] Taihan, "Products: catalog, aluminum conductors," available online at <http://www.taihan.com/en/product/catalog.asp>
- [30] B. Hasche, "General statistics of geographically dispersed wind power," available online at <http://onlinelibrary.wiley.com/doi/10.1002/we.397/abstract>
- [31] Open energy information, "Commercial and residential hourly load profiles for all TMY3 locations in the United States," available online at <http://en.openei.org/datasets/dataset?sectors=buildings&page=2>.
- [32] NREL, "Solar power data for integration studies datasets : California," available online at http://www.nrel.gov/electricity/transmission/solar_integration_methodology.html.
- [33] Energyonline, "CAISO: Average price," available online at <http://www.energyonline.com/Data/GenericData.aspx?DataId=20&CAISO>.
- [34] Kemet engineering center, "Sodium-Sulfur Batteries and Supercapacitors," available online at <https://ec.kemet.com/knowledge/sodium-sulfur-batteries-and-supercapacitors>.
- [35] S. Boyd, "Convex optimization II," Stanford University. Available online at <http://www.stanford.edu/class/ee364b/lectures.html>
- [36] M. Grant and S. Boyd, *CVX: Matlab software for disciplined convex programming, version 1.21*, <http://cvxr.com/cvx/>, Apr. 2011.



Katayoun Rahbar received her B.Sc degree from Shahid Beheshti University, Tehran, Iran, and the Ph.D. degree from National University of Singapore, Singapore, all in electrical engineering, in 2010 and 2016, respectively. She is currently a research fellow in Solar Energy Research Institute of Singapore (SERIS). Her research interests include energy management in microgrids, renewable energy, smart grids, and convex optimization.



Chin Choy Chai received the Ph.D. and B. Eng. degrees, both in electrical engineering, from the National University of Singapore (NUS) in year 1999 and 1995, respectively. He was a recipient of the NUS Research Scholarship from 1995 to 1998. He has joined the Institute for Infocomm Research, (formerly known as Centre for Wireless Communications, and Institute for Communications Research) in 1998, which is a research institute of the Agency for Science, Technology and Research (A*STAR), Singapore. He is presently a Scientist

and the Deputy Department Head (Research) in their Smart Energy and Environment Department, and the Principle Investigator of research and development projects on demand side management. From 2001 to 2012, he also served as an adjunct assistant professor, and conducted postgraduate courses in the Department of Electrical and Computer Engineering, NUS. His current research interest is in wireless MIMO relay, wireless fading channel models, digital modulation and detection, transmission rate and power control, optimization on load shedding and energy scheduling in smart grids, and demand-side management. He also provides regular voluntary editorial services to IEEE and IEE journals, and serves as technical program member and session chair for IEEE conferences, on the subjects of wireless communications and smart grids.



Rui Zhang (S'00-M'07-SM'15) received the B.Eng. (first-class Hons.) and M.Eng. degrees from the National University of Singapore, Singapore, and the Ph.D. degree from the Stanford University, Stanford, CA, USA, all in electrical engineering, in 2000, 2001, and 2007, respectively. From 2007 to 2010, he worked with the Institute for Infocomm Research, ASTAR, Singapore, where he now holds a Senior Scientist joint appointment. In 2010, he joined the Department of Electrical and Computer Engineering, National University of Singapore, where he is now

an Associate Professor. He has authored over 250 papers. His research interests include energy-efficient and energy-harvesting-enabled wireless communications, wireless information and power transfer, multiuser MIMO, cognitive radio, UAV-assisted communications, wireless surveillance, and optimization methods. He has served for over 30 international conferences as TPC Co-Chair or Organizing Committee Member, and as the guest editor for several special issues in IEEE journals. He has been an elected member of the IEEE Signal Processing Society SPCOM and SAM Technical Committees, and served as the Vice Chair of the IEEE ComSoc Asia-Pacific Board Technical Affairs Committee. He is an Editor for the IEEE TRANSACTIONS ON WIRELESS COMMUNICATIONS, the IEEE TRANSACTIONS ON SIGNAL PROCESSING, the IEEE JOURNAL ON SELECTED AREAS IN COMMUNICATIONS (Green Communications and Networking Series). He has been listed as a Highly Cited Researcher (also known as the Worlds Most Influential Scientific Minds), by Thomson Reuters in 2015. He was the co-recipient of the Best Paper Award from the IEEE PIMRC in 2005, and the IEEE Marconi Prize Paper Award in Wireless Communications in 2015. He was the recipient of the 6th IEEE Communications Society Asia-Pacific Region Best Young Researcher Award in 2011, and the Young Researcher Award of the National University of Singapore in 2015.